IEICE TRANS. INF. & SYST., VOL.E92–D, NO.3 MARCH 2009

PAPER

Segmentation of Arteries in Minimally Invasive Surgery Using Change Detection

Hamed AKBARI[†a)], *Nonmember*, **Yukio KOSUGI**[†], *Member*, *and* **Kazuyuki KOJIMA**[††], *Nonmember*

SUMMARY In laparoscopic surgery, the lack of tactile sensation and 3D visual feedback make it difficult to identify the position of a blood vessel intraoperatively. An unintentional partial tear or complete rupture of a blood vessel may result in a serious complication; moreover, if the surgeon cannot manage this situation, open surgery will be necessary. Differentiation of arteries from veins and other structures and the ability to independently detect them has a variety of applications in surgical procedures involving the head, neck, lung, heart, abdomen, and extremities. We have used the artery's pulsatile movement to detect and differentiate arteries from veins. The algorithm for change detection in this study uses edge detection for unsupervised image registration. Changed regions are identified by subtracting the systolic and diastolic images. As a post-processing step, region properties, including color average, area, major and minor axis lengths, perimeter, and solidity, are used as inputs of the LVQ (Learning Vector Quantization) network. The output results in two object classes: arteries and non-artery regions. After post-processing, arteries can be detected in the laparoscopic field. The registration method used here is evaluated in comparison with other linear and nonlinear elastic methods. The performance of this method is evaluated for the detection of arteries in several laparoscopic surgeries on an animal model and on eleven human patients. The performance evaluation criteria are based on false negative and false positive rates. This algorithm is able to detect artery regions, even in cases where the arteries are obscured by other tissues.

key words: *change detection, laparoscopy, minimally invasive surgery, artery segmentation, learning vector quantization*

1. Introduction

As an alternative to the large incision and body cavity opening required in open surgeries, laparoscopic surgery requires only a few small incisions to insert a laparoscope and other devices. For accurate performance in these minimally invasive procedures, surgeons rely almost completely on a 2D visual monitor. In endoscopic and the laparoscopic procedures, however, the lack of tactile sensation and 3D visual feedback make it difficult to identify a blood vessel's position intraoperatively. For example, in open surgery, the bulge of an artery can change the contour of the overlying tissue, which, in open surgeries, can be seen or even felt by the surgeon. The surgeon can also feel for vessel elasticity with this surgical procedure. In contrast, in laparoscopic procedures, surgeons almost always face the problem of detecting and localizing blood vessels, whether trying to avoid them or to allow for their ligation.

Injury to major vessels in laparoscopic surgery is a serious and life-threatening complication that has been previously reported and reviewed by many different groups [1]–[6]. Differentiation of arteries from other structures and the ability to independently detect them has a variety of potential applications in the head, neck, lungs, heart, abdomen, and lower extremities. It could improve the differentiation and localization of anatomic structures and allow for the assessment of physiologic features, such as perfusion. Several diseases where artery-vein discrimination is potentially useful include pulmonary hypertension, pulmonary embolism, coronary artery disease, hepatic cirrhosis, portal vein thrombosis, renal hypertension, lower extremity occlusive disease, and lower extremity deep venous thrombosis. Visualization of both arterial and venous structures in the same image has the potential to provide additional valuable information; for example, it could allow surgeons to evaluate venous conduits for peripheral vascular surgery. In addition, the anatomic relationship between arteries and veins in tumors may be useful in the study and management of cancer [7]. Proper localization of the cystic artery is of the utmost importance in laparoscopic cholecystectomy because safe stapling of this artery is needed for visualization of the operating surgical field and proper alignment of the biliary ducts and hepatic arteries [8].

A variety of methods have been developed for evaluation of the vascular system, such as laser Doppler Flowmetry (LDF), color Doppler ultrasonography [9], speckle methods, optical coherence Doppler tomography (OCDT) [10], functional imaging and monitoring of blood oxygenation [11], X-ray angiography, computed tomography angiography (CTA), and magnetic resonance angiography (MRA) [9]. Optical methods are attractive for identifying arteries in laparoscopic surgery mainly because light delivery to and from tissue can be accomplished via fiber optics [1]. As arteries are the only pulsatile objects in our system, we use this property to detect arteries or differentiate them from veins. In this paper, an optical change detection method for pulse sensing is developed and evaluated on an animal model and in eleven human surgery cases.

2. Materials and Methods

A medical laparoscope system by Olympus with light source unit CLV-U40 was used in this study. The dynamic range of the pixel in each color channel was 8 bits, and the result-

Manuscript received April 18, 2008.
Manuscript revised November 5, 2008.

[†]The authors are with the Department of Mechano-Micro Engineering, Tokyo Institute of Technology, Yokohama-shi, 226–8502 Japan.
[††]The author is with the School of Medicine, Tokyo Medical and Dental University, Tokyo, 113–8519 Japan.
a) E-mail: akbari.h.aa@m.titech.ac.jp

DOI: 10.1587/transinf.E92.D.498

ing image size was 480 × 720 pixels. Arterial pressure rises and falls because of cyclic heart muscle function (i.e., contraction and relaxation). The maximum and minimum pressures corresponding to cardiac contraction and relaxation are respectively called the "systolic" and "diastolic" pressures. This pressure variation within the artery produces a pulsatile movement, which is observable in any artery and reflects heart activity [12].

A laparoscopic view consists of arteries, veins, and other tissues and organs. Although the colors of arteries, veins, and other tissues are quite different because of light scattering by tissue over the vessels, one cannot easily differentiate an artery from a vein or detect a blood vessel that is covered by other tissues. In some instances, the surgeon can detect a blood vessel, but may find it difficult to differentiate an artery from a vein. In this study, we use an artery's pulse to detect arteries that are covered by other tissues and to differentiate between arteries and veins. All arteries that were in the field of the view of the surgeons were evaluated. Artery size ranges from 1–10 mm. The pulse rates in the pig and human were 95–120 bpm (beats per minute) and 65–90 bpm, respectively. The displacement due to the artery's pulse was 1–14 pixels.

The frame rate of the laparoscopic movie was 30 frame/sec. One of the most important issues in arterial pulse detection is sampling time. The input to the change detection algorithm consists of two images. Although a larger number of sample images will result in a more precise output, the use of only two images as algorithm inputs shortens calculation times. To maximize the change between two images, the images were captured during the systolic and diastolic phases. Although it is possible to use an ECG (Electrocardiogram) to trigger the capture time in commercialized systems, an ECG synchronized image was not available in this case due to ethics approval protocols and guidelines. Therefore, we extracted the appropriate frames directly from the laparoscopic movie using the maximum and minimum changes detected between frames in the pig and human. To calculate the change, two frames were first registered via a Fast Fourier Transform (FFT)-based method. The change was then calculated through our change detection method, as explained below. The change that arises from a pulse is additive to any other changes occurring in the region; hence, the maximum change occurs between systole and diastole. The heart rate calculated based on the method of determining the number of successive systoles within a minute exactly matches the heart rate recorded over the same time interval used for image extraction. A pair of diastolic and systolic images is shown in Fig. 1. These images show a 2-pixel vertical and 5-pixel horizontal shift, and small movement of the surgical devices.

An artery's pulse changes the artery shape, enlarging it and/or moving the surrounding tissue. A set of the laparoscopic images of the same scene is given at systolic and diastolic times. We eliminated unreal changes and differentiated changes due to the pulse from those due to surgical interventions. The change mask may result from a combination of underlying factors, including camera motion, noise, illumination variation, non-uniform attenuation, appearance or disappearance of objects, motion of objects relative to the background, and/or shape changes of objects. Generally, there are two types of changes that occur in laparoscopic surgery: those due to motion of the laparoscope and changes due to tissue movement. Tissue movements are either physiological or induced by surgical intervention. Like other types of change detection procedures, it is necessary to register systolic or diastolic images of the same scene captured at different times.

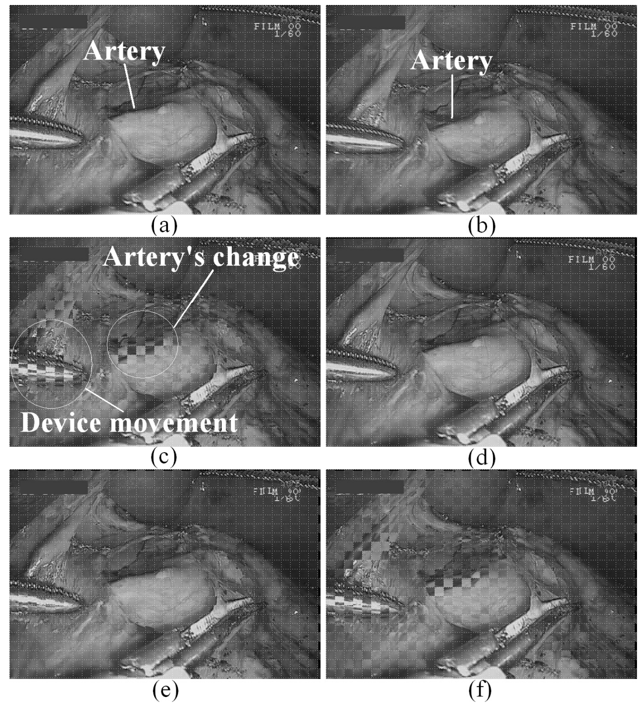

Fig. 1 Laparoscopic images of the LADG procedure in a human, which are inputs for the arterial pulse detection algorithm: (a) systolic image, (b) diastolic image, (c) a checkerboard image created by combining alternating squares from the systolic and diastolic images, (d) the registered systolic image based on the diastolic image using the global affine method, (e) a checkerboard image made by combining alternating squares from the systolic and the registered systolic images. (f) a checkerboard image made by combining alternating squares from the diastolic and the registered systolic images.

2.1 Image Registration

There are several methods to automatically perform the registration: algorithms that directly use image pixel values; algorithms that operate in the frequency domain; algorithms that use low-level features such as edges and corners; and algorithms that use high-level features such as identified objects [13]. To find a more appropriate method for registration, the Wavelet-Modulus Maxima algorithm, Fast Fourier Transform (FFT) method, Morphological Pyramid Image Registration method and a nonlinear local registration method were compared to cover different registration classes.

The Wavelet-Modulus Maxima (WMM) method uses image pixel values in the following manner [14]: control points are extracted from the local modulus maxima of the wavelet transform and applied to the input and base images, after which the images undergo two levels of wavelet decomposition. The correlation coefficient is used as a measure of similarity. The points corresponding to best pairwise fit among all pairs of feature points are taken as the actual control points. Registration is performed using these control points in the base image.

The Morphological Pyramid Image Registration (MPIR) algorithm [15] uses the shape features and an illumination change model to determine the 2D global affine transformation. The correspondences between images can be described by mapping functions with unknown matching parameters. The Levenberg-Marquardt non-linear optimization algorithm is used to estimate these matching parameters. In this approach, intensity mapping function is integrated into a geometric mapping function. This algorithm is capable of measuring the displacement between images subjected to simultaneous translation, rotation, scaling, and shearing.

The nonlinear mapping algorithm that represents a type of elastic deformation was also evaluated because the presence of non-rigid structures and the 3D nature of the abdominal tissues and organs make it highly relevant [16]. This method uses image pixel values directly in space domain. The objective is to map the original image onto the destination image by iteratively moving each portion of the original image. The movement of the original image pixels constitutes a set of shifting vectors. To find the set of shifting vectors, we subdivided the original image to be scanned over the neighboring corresponding point of the destination image. We chose the segment size or division size to be small enough, e.g., 8×8 pixels, to minimize image distortion due to nonlinear displacement of the segment. After the consensus operation, the original image is slightly deformed according to the set of shifting vectors. After several iterations, a nonlinear mapping from the original to the destination image is performed. The network flowchart is illustrated in Fig. 2.

Ultimately, the FFT-based method that operates in the frequency domain was chosen, as it had short computational time and was sufficiently precise. In contrast, the nonlinear local registration method omitted the artery pulse. Unwanted tissue movements caused by surgical devices, were eliminated in post-processing. Table 1 shows a comparison of the different registration methods.

2.2 FFT Based Image Registration

The image registration algorithm used in this paper applies an edge-based method for matching systolic and diastolic images. This algorithm consists of a model combining a 2D affine transformation and an illumination change. Using edges rather than the intensity of the image eliminates details while maintaining shape features. This edge-based registration yielded better results than its intensity-based counterpart did in our experiment.

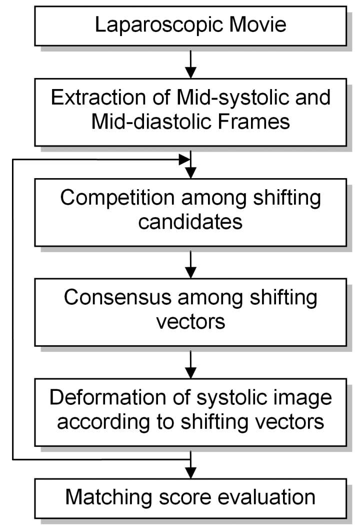

Fig. 2 Procedure for nonlinear elastic mapping.

For the first step, we use Canny's method for edge detection [17]. For the Gaussian filter, sensitivity thresholds of 0.1 and 0.4, and a standard deviation of 1 were chosen based on the best results obtained for registration. False edges can be detected by recognition of the edges of glare and surgical equipments used in the laparoscopy. Thus, the edges detected around pixels located in these regions of systolic or diastolic images are eliminated. In order to prevent false edge detection due to non-uniform illumination, we applied the registration method to a square (400×400 pixels) in the center of the base image. This region had uniform illumination in most images.

The FFT-based automatic registration algorithm is based on the Fourier shift theorem. When two images differ only by a shift, their Fourier transforms are related by the following equation.

$$F(\xi, \eta) = e^{-j2\xi(x\xi + y\eta)} F1(\xi, \eta) \tag{1}$$

where $F(\xi, \eta)$ and $F1(\xi, \eta)$ are Fourier transforms of two images. The ratio of two images is defined as:

$$R = \frac{F1(\xi, \eta) conj(F(\xi, \eta))}{abs(F1(\xi, \eta)) abs(F(\xi, \eta))} \tag{2}$$

where $conj$ is the complex conjugate and abs is the absolute value. By taking the inverse Fourier transform of R, the resulting function is approximately zero everywhere, except for a small region around a single point. This single point is where the absolute value of the inverse Fourier transform of R reaches its maximum value. The location of this point is exactly the displacement between the two images, which is needed to optimally register in the images [13]. Converting these images from rectangular coordinates (x, y) to log-polar coordinates $log(r, \theta)$ makes it possible to represent both rotation and scaling as shifts. However, computing $log(r, \theta)$ from the original rectangular grid leads to construct

Table 1 The error values and error percentages (error to image size ratio) of different registration methods.

Method	shift (pixel)	Rotation (degree)	Scaling	Time
WMM	0.05 (0.01%)	0.34 (0.09%)	0.01%	10–12 sec
MPIR	0.03 (0.01%)	0.22 (0.06%)	0.01%	30–40 sec
FFT	0.04 (0.01%)	0.32 (0.09%)	0.01%	3–4 sec
Elastic	0.00>(0.00%>)	0.00>(0.00%>)	0.00%>	20–22 min

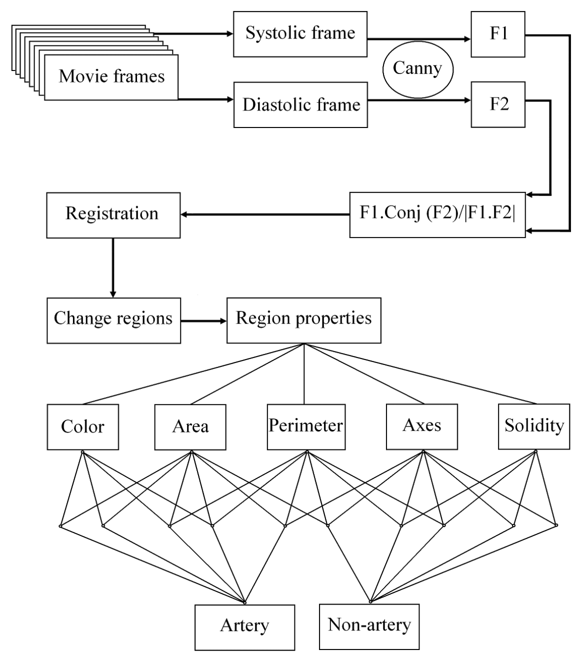

Fig. 3 Flowchart of the artery detection algorithm.

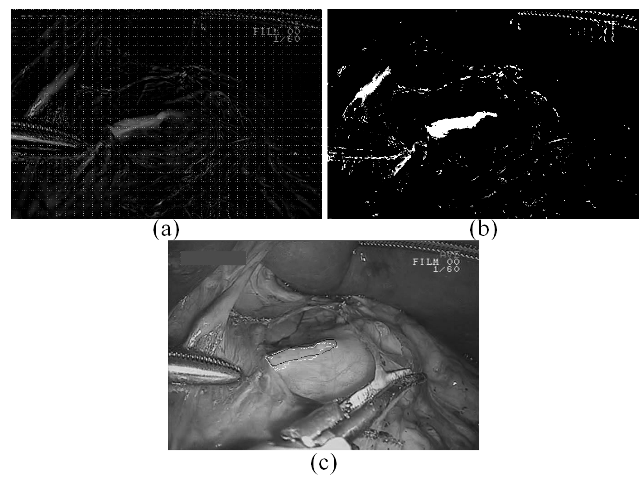

Fig. 4 The changes detected by the global affine method in a human surgery: (a) absolute subtraction values of registered systolic and diastolic images, (b) the detected changes after applying a threshold, (c) the detected artery, using the proposed method, is demarcated with white lines and a hand-created artery region drawn by medical doctors is shown with black lines.

points that do not exactly overlay the points in the original grid [18]. Thus, interpolation is needed to find a value of $abs(F(\xi, \eta))$ on the desired grid. The flowchart and a sample registered systolic image using this method are shown in Figs. 3 and 1, respectively.

2.3 Change Detector

To obtain a change/no-change classification, the difference map was binarized by defining a threshold value. The method applied in this paper is based on a generic methodology for target-detection performance evaluation. Given a threshold value for a change, the proposed method calculates false detection (false positive) and false rejection (false negative) regions using reference image pairs that represent the captured images at times t_1 and $t_2 > t_1$ (i.e., systolic and diastolic images). The reference images differ only in the presence or absence of an artery. For a given threshold value, a distance measure $D(t_1, t_2)$ (i.e., systolic and diastolic images) must be defined. If the threshold is chosen at some value, we can compute the following probabilities:

$$P(FN) = P(\textit{failure to detect}) \qquad (3)$$

$$P(FP) = P(\textit{false detection}) \qquad (4)$$

where P(*) is the probability operator. FN and FP represent false negatives and false positives, respectively. By varying the threshold from zero to some maximum value, a curve of $P(FN)$ versus $P(FP)$ can be determined. We adjusted the threshold to different values for different frames of surgeries, based on average intensity change in each surgery and $P(FN) = 0$. In this way, we could be sure to detect all arteries. Absolute subtraction results for the registered systolic and diastolic images (Fig. 1) before applying threshold are shown in Fig. 4.

2.4 Post-Processing

In laparoscopic images, the changes caused by an artery often arise from the appearance or movement of an artery with predictable characteristics. The changes, therefore, occur within a specific size range with continuous and differentiable boundaries; the change detection algorithm tries to conform the change mask to these expectations. In addition, changes may be induced by surgical instruments and glare, although these should be eliminated.

As a post-processing step, region properties are used to eradicate all changes except that induced by the pulse. Application of LVQ (Learning Vector Quantization) neural networks can enable the system to overcome the complexity of the distribution of regional properties. An LVQ network has a primary competitive layer and a secondary linear layer. The classes learned by the competitive layer are re-

Table 2 The results for image registration of 20 images. The percentage reflects error to image size ratio.

Vertical shift (pixel)		Horizontal shift (pixel)		Rotation (degree)		Scaling	
Range	Error	Range	Error	Range	Error	Range	Error
±45	0.00 (0.00%)	±75	0.01 (0.00%)	±10	0.21 (0.06%)	0.70–0.90	0.01%
±(46–90)	0.03 (0.01%)	±(76–150)	0.03 (0.00%)	±(11-20)	0.23 (0.06%)	0.91–1.10	0.01%
±(91–135)	0.05 (0.01%)	±(151–225)	0.07 (0.01%)	±(21–30)	0.41 (0.11%)	1.11–1.30	0.01%
±(136–180)	0.09 (0.02%)	±(226–300)	0.12 (0.02%)	±(31–40)	0.44 (0.12%)	1.31–1.50	0.02%

ferred to as subclasses and the classes of the linear layer as target classes. The linear layer transforms the competitive layer's classes into target classifications [19]. Color average in a region (mean value of RGB in each region in systolic image), area (number of pixels in each region), major and minor axis lengths (the lengths of the major and minor axes of the ellipse that has the same normalized second central moments as the region), perimeter (number of pixels around the boundary of each region), and solidity (the proportion of pixels in the convex hull that are also in the region) are inputs of the network [20]. These properties were chosen based on the best results obtained in post-processing. The output results in two object classes: arteries and non-artery regions. Data from 40 regions (blood vessel and non-blood vessel) were captured for training. All parts of the change detection output algorithm that resulted from glare regions, surgical instruments or changes due to non-uniform illumination were eliminated in this step. As the second post-processing step, a hole-filling filter was applied to maintain consistency in the detected pulses.

3. Experimental Results

In order to carry out an experimental analysis aimed at assessing the performances of the proposed approach, we used data sets for the laparoscopic surgeries of a pig and eleven human patients. The performance of this technique was evaluated for the detection of arteries and the ability to differentiate between arteries and veins in laparoscopic surgery. The following surgeries were carried out: a pig's abdomen; five laparoscopy-assisted Billroth-I gastrectomies (LADG), one surgery on the rectum of a patient with Hirschsprung disease, two surgeries on the stomach of patients with cerebral palsy, one surgery searching for the testis in a vanishing testis patient, and two splenectomies in individuals with Spherocytosis or Idiopathic Thrombocytopenic Purpura (ITP). The blood vessels were selected from different parts of the stomach, intestine, peritoneum, and other tissues and from superficial and deeper vessels. The images covered different shapes of vessels in laparoscopic procedures.

3.1 Evaluation of the Registration Method

We first evaluated the performance of the registration method, which was applied in this work for the elimination of affine changes. Twenty random images were captured from laparoscopic surgery. From each image, a new image was prepared by shifting the original image (base image) by a defined number of columns and rows, by rotating, and/or by scaling the image with pre-defined values of rotation angle and scale. In other words, these new images underwent a combination of shifting, rotating, and scaling. Then, the method was applied to reconstruct the values of shift, rotation, and scale. The computed results matched almost exactly the known values, which are shown in Table 2. This table shows that even when images are distorted by a combination of shifting, scaling and rotation, our method is able to accurately detect each transformation.

A pair of systolic and diastolic images during the LADG procedure in humans is shown in Fig. 1 (a) and (b). Figure 1 (c) was created by combining alternating squares from systolic and diastolic images. It therefore has the clearest difference between mosaic patterns and contains all changes. Figure 1 (d) shows the registered systolic image based on the diastolic image using the global affine method. Figure 1 (e) was made by combining alternating squares from the systolic and the registered systolic images. It shows only rigid movements in these images; as mentioned previously, this motion was 2 vertical pixels and 5 horizontal pixels. It therefore has a lesser mosaic pattern compared to Fig. 1 (c), which is evident when examining the edges of the surgical forceps in left side and upper left corner near the image text. Figure 1 (f), a checkerboard image, was made by combining alternating squares from the diastolic and registered systolic images. The mosaic pattern in Fig. 1 (f) is reduced compared to Fig. 1 (c) that is clearer in the tissue edges. For example, there is a clear mosaic pattern in the upper left corner of Fig. 1 (c), while that region is smooth in Fig. 1 (f).

Secondly, the global affine method was compared to the local elastic method. Twenty pairs of systolic and diastolic images with an artery were selected, and the two methods were applied in each case. The results show that, although registration was better for the local elastic method, the change would eventually be lost since it would, unfortunately, register a change caused by a real pulse back to its previous shape. In other words, an artery's pulse is considered a local change, and the local registration method would cause the change to return to its previous shape. Moreover, twenty images without an artery or other changes due to surgical intervention were captured. In these situations, the results between the two methods were rather similar. The global method was found to be able to register changes due to respiration, similar to the elastic method. Figure 5 shows a registered systolic image using this method as well

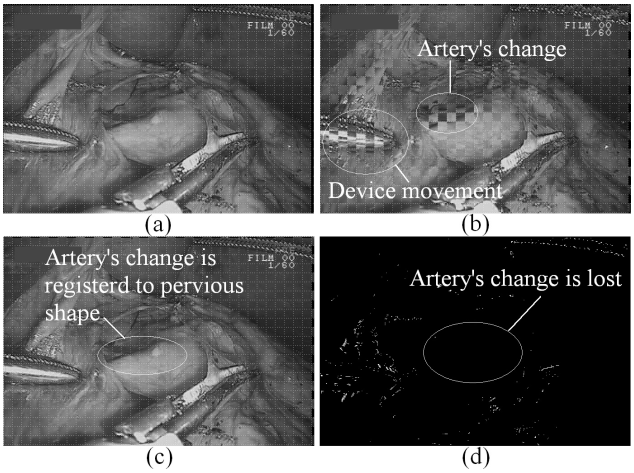

Fig. 5 Local elastic registration in a human surgery case: (a) the registered systolic image based on the diastolic image using the local elastic method, (b) a checkerboard image made by combining alternating squares from the systolic image and the registered images, (c) a checkerboard image made by combining alternating squares from the diastolic image and the registered images, (d) the detected changes after applying the threshold.

as the subtraction of the diastolic image and registered image. The only advantage of the local elastic method was for assessing changes due to surgical interventions. This method could correct such changes only when the changes were not very big. However, we were able to eliminate such changes through post-processing. Therefore, we used the global affine method, which required a lower computational time and did not eliminate pulses.

3.2 Evaluation of Artery Detection

Eighty sequential pair images were extracted from twelve laparoscopic surgeries. Determination of the vascular distribution and differentiation between arteries and veins was done by two medical doctors using a drawing program. These hand-created maps were used as the reference maps in the evaluation. Figure 4 shows a sample of a hand-created map and a detected artery in a laparoscopic image. Both the measurements on the detection of the artery and the ability to differentiate between arteries and veins were evaluated with respect to hand-created maps. The performance criteria for blood vessel detection were the false negative rate (FNR) and false positive rate (FPR). Because, in most cases, arteries were covered by other tissues and medical doctors could only confirm the presence of an artery but not its exact margins, we only evaluated the presence or absence of an artery. In those cases in which arteries were covered by other tissues, the presence of an artery became clear in the subsequent surgical frames. Partial overlap between the hand-created map and the algorithm were accepted if more than 50% of the region matched.

For regions identified as non-artery regions, a false negative signified that the region was identified as an artery region on the hand-created map. The FNR was defined as the number of false negatives divided by the total number of arteries on the hand-created map. For regions identified as artery regions, a false positive signified that the region was identified as a non-artery region on the hand-created map. The FPR was defined as the number of false positive pixels divided by the total number of non-vessel pixels in the hand-created map. Note that the FNR was based on the number of regions, whereas the FPR was based on pixel counts. A region-based calculation of FPR did not make sense because the lack of non-vessel regions would make yield a divide-by-zero error.

Table 3 Results for the proposed method for artery detection during laparoscopy.

	FPR	FNR	Specificity	Sensitivity
Simple detection	10%	0%	90%	100%
Combined results	4%	0%	96%	100%

In each image, blood vessels can vary in shape, size, or orientation. The shapes of vessels can resemble a circle, ellipsis, pipeline, or bifurcation. Each image contained zero to several blood vessels. Table 3 shows the FPR and FNR values of the eighty pairs of laparoscopic images tested. For these paired laparoscopic images, the FPR value showed a specificity of 90% for detecting arteries and the FNR value revealed a sensitivity of 100% for detecting the arteries. To increase the accuracy, we combined the results from three systolic images for each diastolic image, using the three serial systolic images that followed a given diastolic image. If two of the three results yielded an artery region, a true artery was considered as identified. This method was evaluated for twenty series of serial images, and was shown to improve the specificity and sensitivity to 96% and 100%, respectively (Table 3). The computational time was about 6–7 seconds using Matlab software on a 3.6 GHz computer with a 2 GB RAM.

4. Discussion

The recognition and localization of blood vessels to prevent accidental perforations is a major concern in laparoscopic surgery. In almost all minimally invasive surgeries, physicians face the problem of detecting and localizing blood vessels, either in order to avoid them or to ligate them. Currently, different advanced methods are applied in laparoscopic surgeries for the accurate detection of blood vessels and their anatomical features, and for differentiation between arteries and veins. However, current methods are complicated, time consuming, and require expensive and highly technical medical equipment and expertise. As such, they are not suitable for ordinary laparoscopic surgery [21], [22]. In this study, we have evaluated a method for artery detection that does not call for any extra equipment. It is compatible with any ordinary laparoscopic set and can display the artery region in the field of operation.

The algorithm was able to detect arteries with 90% specificity. This means that only 10% of the detected regions were falsely considered to represent an artery. To limit the number of false change detections, a method utilizing three serial results was applied. As a result, the specificity improved to 96%, leaving only a 4% false positive rate. The sensitivities for the single image pair comparison and the serial image comparison were both 100%. Hence, all arteries were correctly detected both in the two-image and in the serial image comparison.

This method can be useful in laparoscopic surgery because it is important to be mindful of vessels. It would also enable a surgeon to be more vigilant during the surgery if he or she notices that there may be a vessel in a particular region. The method is able to continuously detect arteries without interrupting the laparoscopic surgery. In contrast, all of the previously implemented methods require the surgeon's attention to a special region and use highly technical equipment to detect arteries or to differentiate between arteries and veins.

Comparing this work to our previous report [1], we have demonstrated an increase in the sensitivity to 100% (from 95%), and the specificity has increased to 96% (from 92%). In addition, this work uses several different laparoscopic surgeries occurring in different patients, compared to the use of simulated data and the limited number of surgeries (only 2) used in the previous report [1]. It may be possible to decrease the calculation time using super computers or parallel processing. Our method enables the surgeon to see the detected arteries on the monitor during the surgery. It is also possible to convert the output image into an audio signal, which can emit an audio alarm if the surgeon is approaching an artery. If the location of an artery region is known, it will be possible to alert the surgeon whenever a surgical tool enters this region without interfering with other activities.

5. Conclusion

In this paper, a new blood vessel detection method is presented that can extract arteries covered with fat or other tissues. It is an effective method for artery detection, while suppressing veins and other tissues. One of the advantages of this method is its short computational time, which is needed in laparoscopy. The method is potentially useful in laparoscopic surgery, as watching for vessels is important in these procedures, and may be applied in combination with standard procedures while cautioning the surgeon notices to be more vigilant when it is determined that there may be a vessel in a certain region. Further optimization of this algorithm requires experiments with additional types of surgeries; the algorithm also needs to be tested in real time on more experiments in vessel region extraction during laparoscopic procedures. Implementation of automatic artery detection will provide an opportunity for extensive clinical use. Based on clinical validation results, researchers will be able to ascertain the place this technology can have among other advanced tools for the routine detection of arteries, especially in cases of anatomical variations.

References

[1] H. Akbari, Y. Kosugi, and K. Kihara, "A novel method for artery detection in laparoscopic surgery," Surg Endosc, vol.22, pp.1672–1677, July 2008.

[2] J. Fruhwirth, G. Koch, H.J. Mischinger, G. Werkgartner, and N.P. Tesch, "Vascular complications in minimally invasive surgery," Surg. Laparosc. Endosc., vol.7, no.3, pp.251–254, June 1997.

[3] A.G. Nordestgaard, K.C. Bodily, R.W. Osborne, and J.D. Buttorff, "Major vascular injuries during laparoscopic procedures," Am. J. Surg., vol.169, no.5, pp.543–545, May 1995.

[4] R. Guloglu, S. Dilege, M. Aksoy, O. Alimoglu, N. Yavuz, M. Mihmanli, and M. Glumen, "Major retroperitoneal vascular injuries during laparoscopic cholecystectomy and appendectomy," J. Laparoendosc. Adv. Surg. Tech. A., vol.14, no.2, pp.73–76, April 2004.

[5] R.M. Soderstrom, "Injuries to major blood vessels during laparoscopy," J. Am. Assoc. Gynecol. Laparosc., vol.3 (4, Supplement), p.S47, Aug. 1996.

[6] R.M. Soderstrom, "Injuries to major blood vessels during endoscopy," J. Am. Assoc. Gynecol. Laparosc., vol.4, no.3, pp.395–398, May 1997.

[7] T. Lei, J.K. Udupa, P.K. Saha, and D. Odhner, "Artery-vein separation via MRA-An image processing approach," IEEE Trans. Med. Imaging, vol.20, no.8, pp.689–703, Aug. 2001.

[8] Z. Glavic, L. Begic, and R. Rozman, "A new device for the detection and recognition of blood vessels in laparoscopic surgery," Surg. Endos., vol.16, pp.1197–1200, Aug. 2002.

[9] J.S. Suri and S. Laxminarayan, Angiography and plaque imaging, pp.302–313 and p.512, CRC Press, Florida, 2003.

[10] Z. Chen, Y. Zhao, S.M. Srinivas, J. Stuart Nelson, N. Prakash, and R.D. Frostig, "Optical Doppler tomography," IEEE J. Sel. Top. Quantum Electron., vol.5, no.4, pp.1134–1142, July/Aug. 1999.

[11] H. Liu, A.H. Hielscher, F.K. Tittel, S.L. Jacques, and B. Chance, "Influence of blood vessels on the measurement of hemoglobin oxygenation as determined by time-resolved reflectance spectroscopy," Med. Phys., vol.22, pp.1209–1217, Aug. 1995.

[12] A.C. Guyton and J.E. Hall, Textbook of medical physiology, pp.221–233, W.B. Saunders, Philadelphia, 1991.

[13] B.S. Reddy and B.N. Chatterji, "An FFT-based technique for translation, rotation, and scale-invariant image registration," IEEE Trans. Image Process., vol.5, no.8, pp.1266–1271, Aug. 1996.

[14] R. Sharman, J.M. Tyler, and O.S. Pianykh, "A fast and accurate method to register medical images using Wavelet Modulus Maxima," Pattern Recognit. Lett., vol.21, pp.447–462, June 2000.

[15] Z. Hu and S.T. Acton, "Morphological pyramid image registration," Image Analysis and Interpretation, Proc. 4th IEEE South West Symposium, pp.227–231, April 2000.

[16] Y. Kosugi, M. Sakamoto, M. Fukunishi, W. Lu, T. Doihara, and S. Kakumoto, "Urban change detection related to earthquakes using an adaptive nonlinear mapping of high-resolution images," IEEE Geoscience and Remote Sensing Letters, vol.1, no.3, pp.152–156, July 2004.

[17] J. Canny, "A computational approach to edge detection," IEEE Trans. Pattern Anal. Mach. Intell., vol.PAMI-8, no.6, pp.679–714, Nov. 1986.

[18] H. Xie, N. Hicks, G.R. Keller, and H. Huang, "An IDL/ENVI implementation of the FFT-based algorithm for automatic image registration," Int. J. of Computers and Geosciences, vol.29, pp.1045–1055, Oct. 2003.

[19] T. Kohonen, Self-Organization and Associative Memory, 2nd ed., Springer-Verlag, New York, 1988.

[20] R.M. Haralick and L.G. Shapiro, Computer and Robot Vision vol.I, Addison-Wesley, New York, 1992.

[21] J. Perissat, D. Collet, R. Belliard, J. Desplantes, and E. Magne, "Laparoscopic cholecystectomy: The state of art. A report on 700 consecutive cases," World J. Surg., vol.16, no.6, pp.1074–1082, Nov.

1992.
[22] H. Troidl, W. Spangenberger, R. Langen, A. Al-Jaziri, E. Eypasch, E. Neugebauer, and J. Dietrich, "Laparoscopic cholecystectomy: Technical performance safety and patient's benefit," Endoscopy, vol.24, no.4, pp.252–261, May 1992.

Hamed Akbari was born in 1973. He received his M.D. from Tehran University of Medical Science in 2000, M.Sc. in Biomechanical Engineering in 2004, and Ph.D. in Biomedical Engineering from Tokyo Institute of Technology in 2008. He has worked for more than 2 years as a clinician and also has teaching experience at Kar University in Tehran. Since October 2008, he has been working as a postdoctoral fellow at the Tokyo Institute of Technology. His field of research is medical signal and image processing.

Yukio Kosugi received M.S. and Dr. Eng. degrees from the Tokyo Institute of Technology in 1972 and 1975, respectively, both in electronics. He is currently a professor at the Interdisciplinary Graduate School of Science and Engineering, Tokyo Institute of Technology, and is also serving as a visiting professor at Tsukuba Advanced Research Alliance of Tsukuba University. His research interests include information processing in the nervous system and neural network-aided image processing in medical and remote sensing fields.

Kazuyuki Kojima received his M.D. degree from Gunma University in 1987. He is currently a professor at the Gastrointestinal Surgery Department, Tokyo Medical and Dental University. His research interests include objective estimation of less invasive laparoscopic surgery and the influence of laparoscopic devices on nerves.